

Study of Nonlinear Lumped Element Transmission Lines for RF Generation*

Fernanda Sayuri Yamasaki¹, José Osvaldo Rossi, Joaquim José Barroso

Associated Plasma Laboratory
National Institute for Space Research
São José dos Campos, Brazil
fernandayamasaki@hotmail.com¹

Abstract – In recent years there has been great interest in the study of nonlinear lumped element transmission lines (NLETs) for high power RF generation. The lumped line accounts for the dispersion effect while its nonlinear elements (Ls or Cs) are responsible for the nonlinearity. Both these line properties acting simultaneously allow the appearing of high frequency oscillations at the output. In particular, the objective of this paper is to study the behavior of these lines for RF generation by means of Spice simulation and comparison to experimental results using a varicap NLET. In future, it is expected that this technique developed here may be useful for the design of NLETs to drive RF antennas in compact space applications.

Keywords – ceramic capacitor; nonlinear component; RF generation; soliton; varactor diode.

I. INTRODUCTION

Motivated by two scientific works there has been a great interest in the study of nonlinear lumped transmission lines (NLETs) for high power RF generation. The first one [1], a ferrite NLET produced 20 MW RF power peak with 20% efficiency at 1.0 GHz. The second one [2], a ceramic capacitive NLET provided 60 MW RF power peak in the 100–200 MHz range. However, line dielectric losses in the ceramic limited the output frequencies below 200 MHz [3]. To deal with this problem other works [4]–[6] have modeled these lines using numerical programs as the NLET analytic solution cannot be used to predict the exact equation for an input rectangular pump pulse. Normally, for Spice software a varicap NLET is used since the diode junction capacitance varies with the inverse of the reverse voltage applied. Therefore, the aim of this work is to study the behavior of these varicap lines by using Spice circuit simulations and comparing them to experimental results for model validation.

II. NLET OPERATION THEORY

When an input pulse is injected into a dispersive lumped LC line it propagates down along the line length with a velocity given by $c = 1 / (LC)^{1/2}$. If the line is nonlinear with variable capacitance as shown in Fig.1 the portion of the pulse with higher amplitude will travel faster than its lower initial

amplitude as C decreases with increasing voltage. In this way, the pulse peak catches up with the low voltage amplitude, forming an output shock wave front with a very fast rise time. However, as the line is dispersive the output shortest rise time will be limited by the Bragg cutoff frequency:

$$f_{c0} = 1 / \pi \sqrt{LC(V_{max})} \quad (1)$$

where $C(V_{max})$ is the decreased capacitance at the maximum voltage applied.

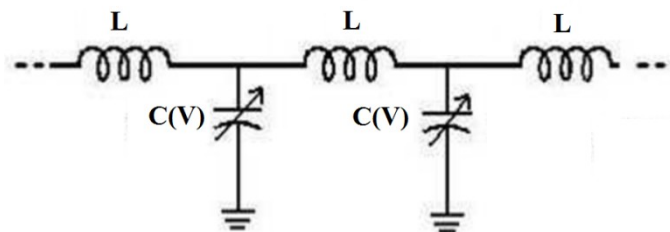


Fig. 1. A section of a capacitive nonlinear transmission line.

One way to understand how soliton oscillations are produced in these lines is shown in Fig. 2. Assuming that a trapezoidal pulse is injected into the line input and the portion of the rise time is approximated by a series of small rectangular pulses with increasing amplitudes and decreasing widths, then each narrow rectangular pulse injected into a nonlinear line generates a soliton that propagates down the line, so that their areas are equally conserved [7]. Solitons can be represented by a squared hyperbolic function, whose amplitude increases with their propagation velocity while the inverse phenomenon is observed for the width. Thus, solitons of higher amplitudes have higher velocities than those of lower amplitudes and they arrive first at the line output. This generates a series of solitons with decreasing amplitudes at the output as shown in Fig. 2.

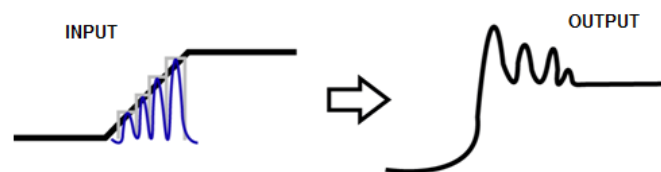


Fig. 2. Soliton generation produced in a NLET.

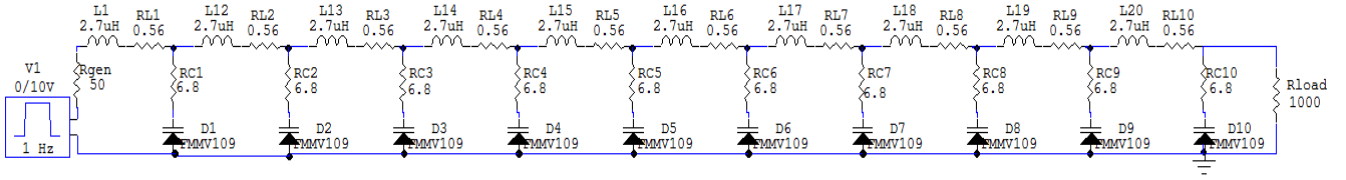


Fig. 3. NLETL schematic circuit using FMMV109 varicap.

A rough estimate for the pulse rise time reduction caused by the LC ladder sections is made by calculating the time delay difference between the lower amplitude portion and the peak of the propagating pulse as [8]:

$$\Delta T = t_{ri} - t_{ro} = n(\sqrt{LC_0} - \sqrt{LC(V_{max})}) \quad (2)$$

where t_{ri} is the input rise time, t_{ro} is the output rise time, n is the number of sections of the line and C_0 is the unbiased capacitance. A more accurate estimation is difficult because of the nonlinearity, but also due to dispersion (phase velocity dependence on frequency). The final rise time of the output compressed pulse (shock wave front) is calculated such as $t_{ro} = t_{ri} - \Delta T$, where t_{ri} is the input pulse rise time with $t_{ri} > \Delta T$. On the other hand, if t_{ri} starts to decrease so that $t_{ri} \approx \Delta T$, t_{ro} cannot decrease to zero as the steepness of the output shock wave would become infinite. Therefore, the pulse rise time reduction is limited ultimately by the lower cutoff frequency of the LC ladder as the propagating pulse cannot be submitted to further sharpening if n tends to a high number and, consequently the spectrum of frequencies from the shock wave is separated since the energy cannot propagate above f_{co} , producing at the output a series of narrow pulses (solitary waves) of high frequency on the order of f_{co} . Therefore, (2) becomes:

$$\Delta T = n(1 - \sqrt{k})\sqrt{LC_0} \approx \pi\sqrt{LC(V_{max})} = \pi\sqrt{k}\sqrt{LC_0} \quad (3)$$

where the nonlinearity factor $k = C(V_{max})/C_0$. Canceling on both sides $\sqrt{LC_0}$ and isolating k obtains:

$$k = \left(\frac{n}{n + \pi}\right)^2 \quad (4)$$

It is noted in (4) that for a large value of n , $C(V_{max})$ is slightly below the value of C_0 , indicating that for a large number of sections n the nonlinearity factor k can be very close to unity, which means that capacitors with more stable capacitance can be used. This explains why in practice it is easier to produce a sufficient number of oscillations (i.e. a train of solitons) with reasonable amplitude output when a NLETL is built with 50 or more sections.

III. EXPERIMENT AND SIMULATION RESULTS

The NLETL was mounted on a phenolite PCB using 10 LC sections with $L = 2.7 \mu\text{H}$ and the FMMV109 varicap as C. Fig. 3 shows the corresponding diagram circuit of the

varicap NLETL, including ohmic losses of L and C (respectively, $RL = 0.56 \Omega$ and $RC = 6.8 \Omega$). The varicap capacitance as function of V is assumed to be given by:

$$C(V) = C_{j0}/(1 + V/V_j)^m \quad (5)$$

where V_j is the diode junction potential and m is the nonlinearity factor. Note that $C = C_{j0}$ for $m = 0$ as expected and generally in many cases $m = 1/2$. From the FMMV109 datasheet, C_{j0} and V_j are assumed to be respectively 61.30 pF and 0.70 V in simulations, while m is the main varicap parameter to be investigated to produce a good fitting between experimental and simulations results. The line is fed by a 50 Ω output impedance pulse generator with 11 V amplitude pump pulse injected with 350 ns duration and 110 ns rise time as shown in Fig. 4 by the experimental result in red. In this case as the input pulse rise time is greater than factor ΔT (of the order of 80 ns with $m = 0.70$ using (5) and (2)) the pulse is compressed at the output as shown in Fig. 5 by the red line, in which it is noticed clearly that the output pulse rise time is reduced to approximately 30 ns.

Figs. 4 and 5 show also the comparison between the Spice corresponding simulations and experimental results using two different circuit simulators (LT-Spice and Circuit Maker - CM). As an example, two different values of m ($= 0.36$ and 0.7) were used to run the simulations. In Fig. 4 it is observed good agreement between simulation and experiment for both values since in any case the 50 Ω generator output impedance is much less than the line impedance given by $Z = \sqrt{L/C(V_{max})}$. Nevertheless, a better fitting between results at output (shown in Fig. 5) is achieved with higher $m = 0.70$ as dispersion effect is much smaller than nonlinearity in this case because of the longer input pulse rise time.

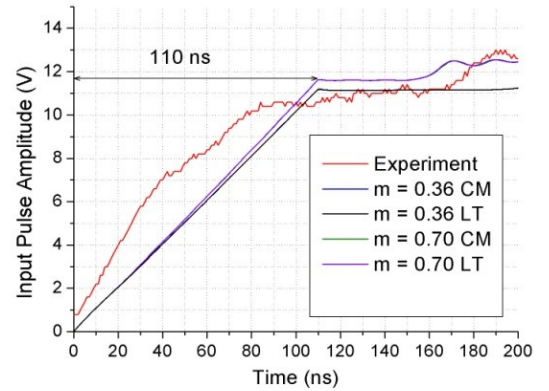


Fig. 4. Pulse sharpening case: input pulse.

IV. CONCLUSIONS AND FUTURE WORK

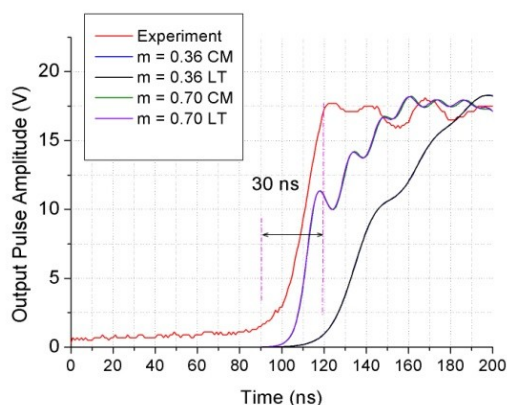


Fig. 5. Pulse sharpening case: output pulse.

On the other hand, using a pulse generator of 30 ns lower rise time so that $\text{tri} < \Delta T$ produces high frequency oscillations on the output pulse amplitude as shown in Fig. 6. The best fitting between simulations and experimental curves were obtained using the same previous line parameters ($C_{j0} = 61.30$ pF and $V_j = 0.70$ V), but with reduced m ($= 0.36$) for a 10 V input pulse amplitude. Note in this case that the stronger line dispersive effect tends to reduce the wave phase velocity, which in turn reduces the factor m . Moreover observe in results of Fig. 6 that f_{co} limits the output rise time to 25 ns approximately as expected and the oscillation frequency obtained at output is on the order of 40 MHz according to (1). Finally, it is verified in the results that equal responses are obtained using LT and CM circuit simulators.

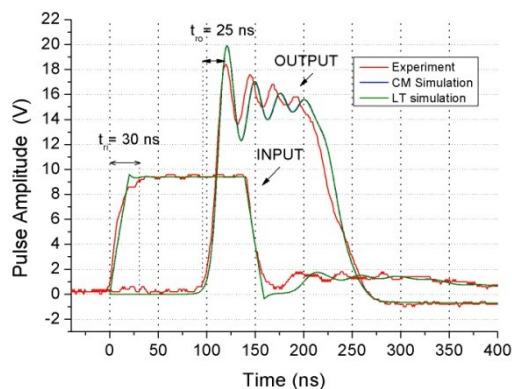


Fig. 6. Input & output pulses for oscillatory case.

In this paper, it was shown that NLETs can be used for pulse sharpening or RF generation depending on the rise time of the input pulse applied. Also the Spice model developed has been validated by comparison between simulations and experimental data using a varicap NLET prototype. However, the small discrepancies observed between the results are probably due to two main factors: 10 % variation of parameter C_{j0} of the varicaps used in the NLET as specified in their data sheet and input pulse approximation by a slow ramp in Spice simulation rather than convex curve as seen in the respective experimental curves in Figs. 4 and 5. As future work, it is intended to replace the varicaps by ceramic capacitors for NLET operation at high power levels and to test a hybrid NLET that is built by using both nonlinear elements (i.e. $L(I)$ and $C(V)$). Finally, it is expected that the techniques and Spice models developed described in this work be helpful in the design of compact NLETs for replacing electronic tubes in space and airborne applications such as telemetry and commands systems of satellites and defense mobile platforms, respectively.

REFERENCES

- [1] B. Seddon, C. R. Spikings, and J. E. Dolan, "RF pulse formation in NLETs" in Proc. of the 2007 16th Int. Pulsed Power Conf., pp.678-681.
- [2] P. M. Brown and P.W. Smith, "High power, pulsed soliton generation at aadio & microwave frequencies", in Proc. of the 1997 11th International Pulsed Power Conf., pp. 346-354.
- [3] P. W. Smith, "Pulsed, high Power, RF generation from nonlinear dielectric ladder networks – performance limits," presented at the 18th IEEE Int. Pulsed Power Conf., Chicago, IL, 2011.
- [4] J. D. Darling & P. W. Smith, "High power RF generation from non-linear delay lines," in Proc. of the 2007 16th Int. Pulsed Power Conf., pp. 472-475.
- [5] J. O. Rossi and P. N. Rizzo, "Study of hybrid nonlinear lines for high power RF generation", in Proc. of the 2009 IEEE Pulsed Power Conf., pp. 46-50.
- [6] N. S. Kuek, A. C. Liew, E. Schamiloglu, and J. O. Rossi, "Circuit modeling of nonlinear lumped element transmission lines including hybrid lines," IEEE Transactions on Plasma Science, vol. 40, n0. 10, pp. 2523-2534, Oct. 2012.
- [7] F.S. Yamasaki, RF generation using nonlinear transmission lines for aerospace applications. M.Sc. Thesis, INPE, Feb. 2012.
- [8] P.W. Smith, Transient electronics – pulsed circuit technology, John Wiley & Sons, West Sussex, England, 2002, pp. 245-249